frontiers | Frontiers in Materials

TYPE Original Research
PUBLISHED 08 October 2025
DOI 10.3389/fmats.2025.1671031

OPEN ACCESS

EDITED BY
Nitish Bibhanshu,
Indian Institute of Technology Ropar, India

REVIEWED BY
Abdalrhman Milad,
University of Nizwa, Oman
Ashish Kumar Gupta,
Oklahoma State University, United States

*CORRESPONDENCE
Uttam U. Deshpande,
uttamudeshpande@gmail.com

RECEIVED 22 July 2025
ACCEPTED 15 September 2025
PUBLISHED 08 October 2025

CITATION
M. S. P, H. J. A, K. A. V, Avalappa MG and Deshpande UU (2025) Effect of cavitation inducers on slurry erosion resistance of HVOF-sprayed stainless-steel coatings. *Front. Mater.* 12:1671031. doi: 10.3389/fmats.2025.1671031

Effect of cavitation inducers on slurry erosion resistance of HVOF-sprayed stainless-steel coatings

Prathap M. S.[1,2], Amarendra H. J.[1], Venugopal K. A.[1], Manjunath G. Avalappa[3] and Uttam U. Deshpande[4]*

[1]Department of Mechanical Engineering, Malnad College of Engineering, Hassan, Karnataka, India, [2]Visvesvaraya Technological University (VTU), Belagavi, Karnataka, India, [3]Mechanical Engineering Department, KLS Gogte Institute of Technology, Belagavi, Karnataka, India, [4]Electronics and Communication Engineering, KLS Gogte Institute of Technology, Belagavi, Karnataka, India

High-Velocity Oxy-Fuel (HVOF) spraying has extensively been used for improving erosion resistance of stainless-steel parts exposed in aggressive conditions. The paper addresses the behavior of wear loss for HVOF-sprayed stainless steel coatings during slurry erosion under conditions with and without a cavitation inducer condition. Slurry erosion experiments with 20-h wear testing at 5-h intervals with measurements were conducted by using silica sand (600 µm) with a 10 wt.% solution of tap water. The findings suggest that the availability of cavitation inducers has a considerable influence on wear resistance, with some of the samples developing an increase in wear loss at shorter times, and others showing lesser material loss over time. Notably, the 20Ni80Cr sample developed an increase in wear loss at 5 h, whereas other samples developed responses at later stages. The research emphasizes the mechanical impact's role in changing erosion mechanisms and offers information on how to optimize HVOF coatings for enhanced durability in industrial use.

KEYWORDS

high-velocity oxy-fuel (HVOF), slurry erosion, cavitation inducers, stainless steel, wear resistance, nickel-chromium alloys

1 Introduction

Components in critical industries such as aerospace, hydropower, automotive, energy, and marine are often exposed to severe erosive environments where reliability and durability are paramount. Turbine blades, pump impellers, valves, and pipelines, for example, operate under continuous slurry or particle-laden flows that accelerate material degradation. While stainless steels are widely used due to their corrosion resistance and cost-effectiveness, they are highly susceptible to surface damage and dimensional loss when subjected to high-velocity erosive impacts. This degradation not only reduces service life but also leads to frequent maintenance, downtime, and high replacement costs.

Surface engineering approaches, particularly High-Velocity Oxy-Fuel (HVOF) spraying, have proven effective in mitigating such challenges. HVOF produces dense, well-adhered coatings with low porosity, superior hardness, and high bond strength, thereby improving resistance to erosion and corrosion (Tian et al., 2022). Over the past decades, HVOF-sprayed metallic and ceramic coatings have been extensively investigated for their ability

to enhance the performance of stainless steels in slurry and particle erosion conditions (Amarendra et al., 2017; Milanti et al., 2014). However, most of these studies emphasize coating microstructure, hardness, or compositional optimization, while largely overlooking the mechanical influences associated with cavitation phenomena.

Cavitation arises from the nucleation and collapse of vapor bubbles in fluid systems, generating localized high-pressure micro jets and shockwaves. When combined with slurry erosion, cavitation accelerates surface fatigue, promotes crack initiation, and causes severe material spallation (Finnie, 1960). In practical systems, cavitation inducers geometrical features or flow disturbances—can significantly intensify these effects by creating localized stress concentrations. Despite its relevance to real operating conditions, the influence of cavitation inducers on erosion performance of HVOF coatings remains insufficiently studied.

Among available coating materials, nickel–chromium (Ni–Cr) alloys are particularly attractive because of their tunable balance between hardness and toughness. Chromium enhances surface stability, hardness, and oxidation resistance, whereas nickel improves ductility and suppresses crack propagation. Existing research has shown that chromium-rich coatings generally perform better under oxidative conditions, while nickel-rich coatings provide improved toughness and impact resistance (Ramanath et al., 2024). Yet, the effect of varying Ni–Cr ratios on slurry erosion performance particularly under cavitationinducing conditions has not been systematically addressed. This knowledge gap limits the rational design of coatings for environments where combined slurry and cavitation erosion mechanisms dominate.

The present study seeks to address this gap by systematically investigating the erosion resistance of HVOF-sprayed stainless steel coatings in the presence and absence of cavitation inducers. Four coating systems were examined: as-received stainless steel (AR), 40Ni60Cr, 50Ni50Cr, and 20Ni80Cr. Wear loss was measured at 5-h intervals over a 20-h test duration to capture both transient and steady-state degradation trends. A 10 wt.% silica sand slurry (200–300 μm particle size) in tap water was used as the erosive medium to replicate aggressive industrial conditions.

The specific objectives of this work are to:

1. Quantify and compare the wear performance of different Ni–Cr compositions under slurry erosion alone and slurry + cavitation conditions.
2. Evaluate the effect of cavitation inducers on the wear loss and mechanism of material degradation.
3. Correlate observed wear trends with microstructural and compositional features using XRD and SEM analyses.

The findings provide new insights into the interplay between slurry erosion, cavitation, and alloy composition. In particular, they establish guidelines for optimizing Ni–Cr coatings to achieve enhanced durability in wear-intensive industrial environments.

2 Literature review

The application of thermal spray coatings in aggressive erosive environments has gained increasing attention due to their potential to enhance the service life of components exposed to slurry erosion and cavitation. Industries such as hydropower, marine, mining, and chemical processing frequently encounter simultaneous corrosion, erosion, and cavitation damage, demanding surface engineering solutions that offer multifunctional protection. Among these, high-velocity oxy-fuel (HVOF) spraying has emerged as a prominent method for depositing erosion-resistant coatings such as Cr, Ni-based alloys, and ceramic-metallic hybrids. This review consolidates key studies that explore cavitation and slurry erosion mechanisms, coating microstructures, and the synergistic effects of erosion and corrosion, with an emphasis on recent advancements (Tian et al., 2022; Amarendra et al., 2017; Milanti et al., 2014).

Erosion and cavitation are major causes of material degradation in systems exposed to high-speed fluids or abrasive particles, such as turbines, pipelines, and marine structures. Finnie (1960) provided one of the earliest theoretical models on the mechanisms of erosion by solid particles, forming the basis for future research. Subsequent study was carried out by Li et al. (1995), where they investigated the synergistic effect of corrosion on the erosion of aluminum in silica slurry, demonstrating how aqueous media accelerated material degradation. Wang et al. (2013) focused on high-temperature erosion of alumina ceramics, showing that temperature increases erosion rate due to softening of surface phases. The dual impact of slurry and cavitation erosion was explored in multiple studies. Santa et al. (2009) supported these findings by demonstrating similar results for thermally sprayed coatings under such combined attack.

Ramesh et al. (2011), Ramesh et al. (2010) studied APS and Ni–P/Si_3N_4 reinforced coatings, respectively, for erosion resistance, both indicating significant wear reduction. Subsequently, Hong et al. (2015) investigated the behavior of WC-10Co-4Cr coatings in saline solutions, finding excellent corrosion and cavitation resistance. Similar findings were reported by Kumar et al. (2017) and Sapate et al. (2021) who studied the effect of coating thickness on erosion resistance. Thakur and Arora (2013) further confirmed that WC-CoCr coatings perform better under slurry than dry erosion. Yang et al. (2018) and Senapati et al. (2022) contributed newer perspectives, showing that NiCrBSi–Cr_3C_2 composite and NiAl composite coatings, respectively, have significant potential for high-erosion environments. Lin et al. (2022) explored cavitation-silt erosion for offshore machinery, emphasizing the multi-factor nature of marine erosion.

Xu et al. (2017) validated the performance of Inconel 625 coatings formed via laser cladding with wire, exhibiting fine microstructure and strong interfacial bonding. Zafar and Sharma (2014) used microwave cladding to deposit WC–12Co layers, finding excellent slurry erosion resistance. Yi et al. (2022) explored a functionally graded ZrN-to-Ti coating, offering a design concept combining multiple material advantages across the coating thickness, contributing to improved erosion behavior.

Grewal et al. (2013a), Grewal et al. (2013b) explored sand concentration as a key factor in slurry erosion, while a CFD-based test rig was designed to better simulate realistic erosion conditions. Vignesh et al. (2019) evaluated the performance of amorphous HVOF coatings under slurry, with promising results. Maurer and Schulz (2014) extended the erosion study to PVD coatings on CFRP, a lightweight composite material, showing that such coatings can also be optimized for wear-critical environments. Suresh Babu et al. (2011) showed that erodent hardness greatly affects erosion behavior, a finding echoed by Santacruz et al. (2019),

who compared martensitic stainless steel to WC-coated steel using jet slurry tests.

Surface modification as a method for improving corrosion and erosion resistance is discussed by Krastev (2012) and Lekka et al. (2005), who promoted electrodeposited composite coatings. Shunin and Kiv (2012) emphasized the potential of nanomaterials for ecological and wear applications. Kumar et al. (2022) tested HVOF-sprayed Al_2O_3–Cr_2O_3 coatings on turbine steels, reporting good erosion resistance even in silt-laden environments. Zhao et al. (2020) developed a composite Ti–C–B_4C coating, exhibiting high hardness and wear resistance.

Seitov et al. (2025) provided a comprehensive review of Cr_3C_2–NiCr HVOF coatings, summarizing improvements in mechanical properties, microstructure, and phase distribution. Algoburi et al. (2024) presented recent findings on WC–NiCrBSi coatings, while Singh et al. (2012) emphasized the practical benefits of WC-10Co4Cr in real-world slurry pipeline systems. Taşan et al. (2005) developed an image-processing technique to assess wear on the asperity level, representing a significant step forward in precise quantification of micro-erosion events.

Through decades of research, from early 1960s work to recent studies using biomimetic, functionally graded, and composite nanostructured coatings, the field of erosion and cavitation resistance has advanced through materials innovation, process optimization, and deeper understanding of synergistic degradation mechanisms. HVOF remains a widely adopted technique due to its flexibility, cost-effectiveness, and superior performance in a wide range of environments. Future research is expected to focus more on multifunctional coatings, environmentally sustainable processes, and data-driven erosion prediction techniques.

The literature underscores that while HVOF-sprayed Cr and Ni-based coatings provide substantial protection against erosion and cavitation, there remains scope for improvement. Future work should focus on:

- Enhancing coating toughness without sacrificing hardness.
- Utilizing multilayer or functionally graded coatings to bridge property mismatches.
- Adopting advanced diagnostics (e.g., digital image analysis) for wear quantification.
- Tailoring coatings for specific environments, especially for marine, geothermal, and mining applications.

3 Experimental setup

3.1 Specimen preparations

3.1.1 Substrate and coating deposition

The base material used was EN 304 stainless steel plates (200 mm × 200 mm × 6 mm), procured from N T Bharat Steels, Bangalore, in annealed condition. The plates were cut to size (Figure 1) and prepared for coating as follows:

- Surface Cleaning: Contaminants were removed using acetone and ultrasonic cleaning for 10 min.
- Grit Blasting: Carried out with alumina particles (mesh size 40) at 0.5 MPa, yielding an average surface roughness of ~6 µm.

FIGURE 1
Ni–Cr coated EN 304 stainless steel specimens prepared for slurry erosion testing (25 mm × 10 mm × 6 mm).

- Preheating: Substrates were preheated to reduce thermal gradients and residual stresses before spraying.

The coatings were applied using a High-Velocity Oxy-Fuel (HVOF) spray system (SX5000, Guangzhou Sanxin Metal S&T Co., Ltd., China). Commercial Ni–Cr alloy powders particle size 15–45 µm were used as coating agents. The powder was axially fed with nitrogen as carrier gas. The optimized HVOF parameters were: oxygen flow 240 L/min, kerosene flow 0.24 L/min, spray distance 200 mm, and powder feed rate 25 g/min. The resulting coatings exhibited a uniform thickness of 150 ± 20 µm.

3.1.2 Test specimen preparation

Following coating, specimens were prepared for slurry erosion testing:

- The coated plates were cut using EDM into rectangular specimens of 25 mm × 10 mm × 6 mm, suitable for the slurry erosion test rig specimen holder.
- Before testing, all specimens were ultrasonically cleaned in ethanol and dried.
- For reproducibility, three replicates were tested under each condition.

3.2 Test setup, test procedure, and parameters

The erosion tests are being carried out using a conventional slurry pot setup, as shown in Figure 2, which has a circular cross section with a diameter of 320 mm and a height of 285 mm. This will allow for sufficient fluid volume to facilitate uniform erosion. The specimen holder consists of upper and lower circular plates with a diameter of 200 mm, designed to secure the CIs and

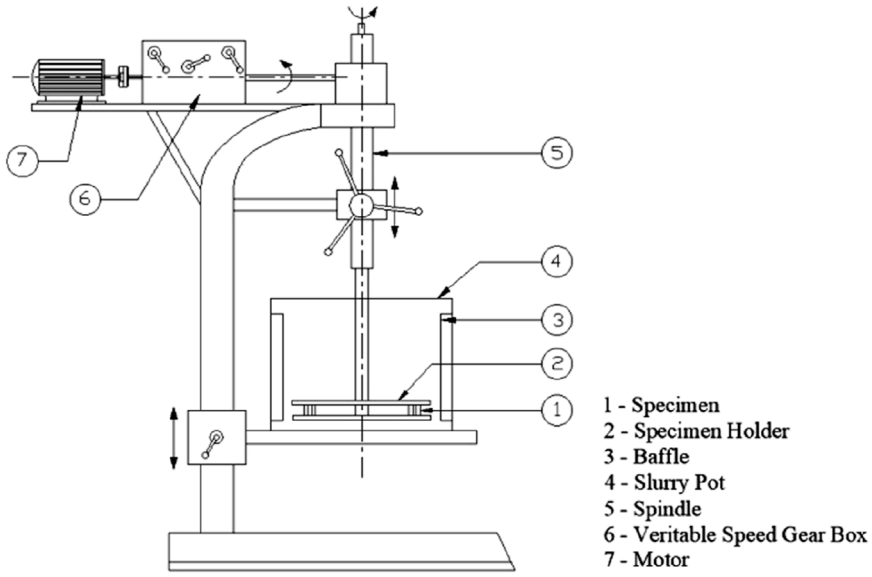

FIGURE 2
Setup of the slurry pot test setup.

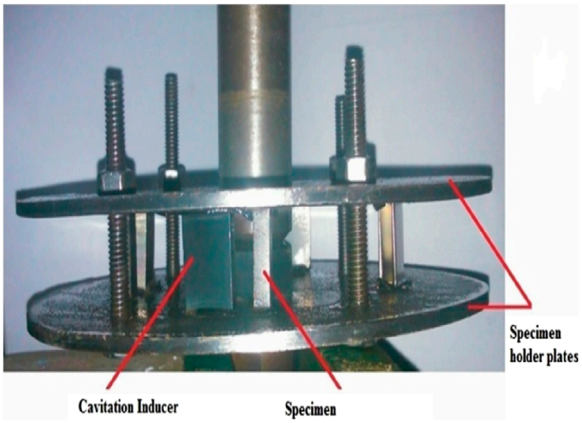

FIGURE 3
Illustrates the arrangement of the specimens and cavitation inducers clamped between two plates, facilitating the evaluation of test specimens under slurry erosion conditions.

specimens firmly in place. The specimen holder is being attached to the test rig spindle via a connecting rod, and the spindle is being powered by a motor operating at 625 rpm with a linear speed of 6.55 m/s.

The slurry pot setup is designed for erosion studies (Figure 3) to ensure the testing conditions remain consistent and can be repeated reliably, allowing for accurate and controlled experimentation. To minimize centrifugal effects and promote effective slurry mixing, four baffle plates are strategically positioned within the pot. Each baffle plate is 30 mm wide and positioned at 90° intervals, helping to disrupt vortex formation and enhance the uniformity of particle distribution within the slurry.

The experiment was conducted for 20 h, with wear measurements recorded every 5 h, allowing sufficient time for measurable material loss due to erosion. This approach enables the tracking of the erosion rate over time and the identification of any potential changes in erosion behaviour, such as stabilization or acceleration of material loss. The erodent material being chosen for the study is silica sand, a widely used abrasive in erosion research due to its high hardness and angular shape, which enhances erosive wear. The 600 μm particle sizes are being utilized to test under severe conditions, ensuring higher material removal due to their kinetic energy. The erosion tests are conducted in a slurry medium composed of tap water, which is serving as the carrier fluid for the abrasive silica sand particles. Tap water, with a pH of 7.0, is widely utilized in industrial and environmental erosion studies due to its neutral properties and accessibility. The slurry concentration is being maintained at 10 wt.%, meaning that 10% of the total slurry weight consists of silica sand particles. This concentration is being selected to ensure adequate particle interaction with the specimen surface.

Each of these test parameters plays a significant role in influencing the erosion behaviour of the specimens:

Rotation Speed (625 rpm – 6.55 m/sec): Affects the velocity of erodent particles and the impact energy upon collision with the specimen surface. Higher speeds generally lead to increased erosion due to higher particle impact forces.

Erodent Size (600 μm): Larger particles are anticipated to induce more intense erosion because of their increased mass, higher impact energy, and the presence of larger, sharper edges.

Slurry concentration: The concentration of abrasive particles in the slurry is increased; there will be more frequent impacts on the material, leading to higher erosion rates. However, if the concentration becomes too high, the particles may start interfering with each other, forming a sort of protective barrier (shielding effect). This reduces the energy transferred by each

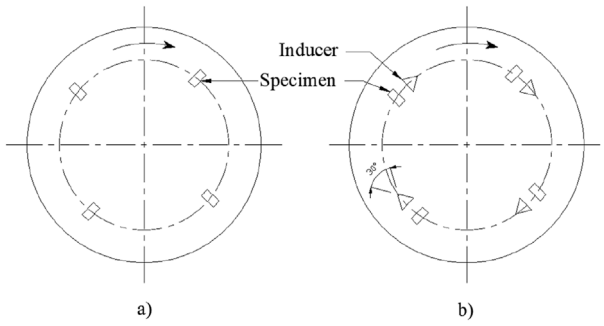

FIGURE 4
Specimen holder, **(a)** without and **(b)** with cavitation inducers.

impact, potentially limiting the effectiveness of the erosion process. Essentially, while more particles can enhance material removal, excessive concentrations might reduce the overall impact of energy, balancing out the erosion effect. Hence, the slurry concentration of 10 wt.% for the present study is adopted.

Test Duration: In this study, a 20-h test duration is implemented to enable the observation of both short-term and long-term erosion characteristics, beginning with initial surface roughening and progressively evolving into a steady-state wear phase.

Weight loss measurements are taken every 5 h to study the short-term erosion characteristics. The periodic measurements are helping to analyze whether the erosion behaviour and to identify influencing factors, such as material hardening, surface roughness changes, or other contributing variables.

Figure 4a depicts the positioning of the specimen without cavitation inducers, meaning only the test specimen is present and undergoing slurry erosion testing. In contrast, Figure 4b displays the specimen setup with cavitation inducers. The triangular cavitation inducers, designed with an apex angle of 30°, are employed to generate localized cavitation effects. Here, the specimens undergo testing for the combined effects of slurry and cavitation erosion. In both configurations, specimens are continuously mounted on a rotating disk to replicate erosive wear conditions. As a result, the developed test ring serves to examine specimens under both slurry erosions alone and the combined impact of slurry and cavitation erosion. Specimens weighed with 0.1 mg precision before and after each test interval (5 h). Cleaned with ethanol and dried before weighing. Three replicate samples were tested for each condition to ensure reproducibility.

4 XRD of test specimen

Phase analysis was performed using an XRD Powder Diffractometer (Proto Manufacturing Ltd., Canada) with Cu Kα radiation (λ = 1.5406 Å). Measurements were carried out in θ–2θ geometry over a range of 20°–90°, with a step size of 0.02°, scanning speed of 2°/min, at 40 kV and 30 mA. The measurement mode was bulk-sensitive, not grazing incidence, ensuring that the data represented the coating phases rather than just the surface.

Reference patterns from the International Centre for Diffraction Data (ICDD) were employed:

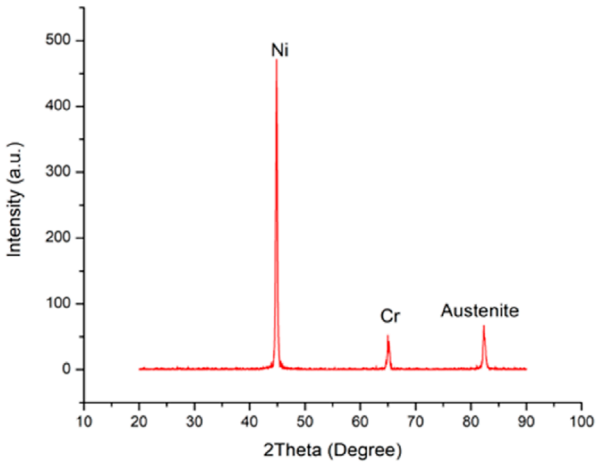

FIGURE 5
XRD pattern of the HVOF-sprayed stainless.

- Ni (JCPDS 04-0850)
- Cr (JCPDS 06-0694)
- Austenite Fe–Ni–Cr (JCPDS 33-0397)

The XRD pattern provides insights into the phase composition of the HVOF-sprayed stainless-steel coating of 50Ni50Cr specimen (See Figure 5). A dominant peak observed in Figure 5 at approximately 45° 2θ corresponds to the Ni phase, indicating that nickel is the primary constituent. Nickel not only enhances corrosion resistance but also stabilizes the austenitic structure. A secondary peak near 65° 2θ is attributed to chromium (Cr), an essential alloying element that contributes to surface passivation and erosion resistance. Another peak around 82° 2θ corresponds to retained austenite, which is known for improving toughness and ductility in metallic systems. The presence of austenite suggests partial preservation of the base stainless-steel structure during the thermal spraying process. The absence of oxide or carbide peaks implies minimal oxidation or secondary phase formation during deposition.

Chromium, as a solid-solution element in Ni-based alloys, does not generally appear as a distinct separate phase; instead, it alters the lattice parameters of the Ni solid solution. This explains the absence of a separate Cr peak. The high-angle austenite peak at ~82° corresponds to the fcc Ni–Cr solid solution and retained austenite from the stainless steel substrate.

The coating exhibits a solid metallic structure dominated by ductile and corrosion-resistant phases. This phase composition is favorable for applications involving slurry erosion and cavitation. The XRD results support the mechanical performance trends observed in wear testing (Akisin et al., 2021).

5 Results and discussions

The wear loss data for different material samples without cavitation inducers shows a clear trend of increasing material degradation over time. Among all the materials tested, the

TABLE 1 Wear loss without Cavitation Inducers.

Sample	Wear loss (mg)			
	5 h	10 h	15 h	20 h
AR	5.000	35.000	46.000	56.000
40Ni60Cr	1.000	18.000	35.000	43.000
50Ni50Cr	2.000	15.000	25.000	29.000
20Ni80Cr	6.000	30.000	38.000	46.000

as-received (AR) sample exhibited the highest wear loss, reaching 56 mg at 20 h, with a sharp increase between 5 h (5 mg) and 10 h (35 mg), indicating poor wear resistance. In contrast, the 50Ni50Cr alloy demonstrated the best performance, with the lowest wear loss of 29 mg at 20 h, suggesting an optimal balance between nickel and chromium that enhances durability. The 40Ni60Cr sample performed better than AR but accumulated 43 mg of wear loss at 20 h, indicating moderate wear resistance. Meanwhile, the 20Ni80Cr sample, despite having a high nickel content, still exhibited 46 mg of wear loss at 20 h, which, although better than AR, was worse than 50Ni50Cr. This suggests that increasing nickel content alone does not necessarily improve wear resistance. Instead, the data indicates that a balanced Ni-Cr composition plays a crucial role in minimizing wear, as seen in the superior performance of 50Ni50Cr. Overall, this analysis highlights the importance of material selection in wear-intensive applications, with 50Ni50Cr emerging as the most wear-resistant alloy, while AR and 20Ni80Cr show significant degradation over time.

Table 1 and Figure 6 illustrate the wear loss (mg) of different materials over time, showing that all samples experience increasing wear as exposure duration increases. AR (As Received) exhibits the highest wear loss, indicating the poorest wear resistance, while 50Ni50Cr consistently shows the lowest wear loss, making it the most durable material. 40Ni60Cr and 20Ni80Cr demonstrate intermediate wear resistance, with 20Ni80Cr wearing slightly more than 40Ni60Cr over time. The steep initial increase in AR's wear suggests rapid material degradation, whereas 50Ni50Cr maintains a lower and steadier wear rate. Overall, 50Ni50Cr is the best-performing material, while AR has the least resistance to wear.

5.1 Wear loss with cavitation inducers

The wear loss data for different material samples in the presence of cavitation inducers reveals notable differences in material performance compared to the condition without cavitation inducers, and the same is dissipated in Table 2. All samples experience wear progression over time, but the impact of cavitation inducers varies across different compositions. The as-received (AR) sample continues to exhibit significant wear loss, reaching 48 mg at 20 h, though this is lower than its 56 mg wear loss in the non-cavitation test, suggesting a slight reduction in material degradation. The 40Ni60Cr sample, which had 43 mg of wear loss at 20 h without cavitation, shows similar wear behavior with cavitation inducers, accumulating 42 mg of wear loss, indicating that cavitation does not drastically affect its wear resistance.

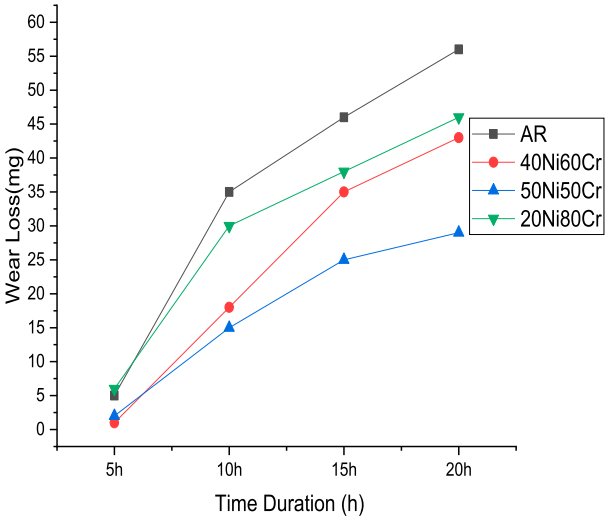

FIGURE 6
Variation of wear loss without cavitation inducers.

TABLE 2 Wear loss with Cavitation Inducers.

Sample	Wear loss (mg)			
	5 h	10 h	15 h	20 h
AR	6.000	26.000	40.000	48.000
40Ni60Cr	6.000	26.000	35.000	42.000
50Ni50Cr	3.000	16.000	26.000	34.000
20Ni80Cr	8.000	24.000	36.000	44.000

The 50Ni50Cr alloy remains the best-performing material, with the lowest wear loss of 34 mg at 20 h, slightly higher than its 29 mg wear loss in the absence of cavitation, suggesting that while cavitation slightly increases its degradation, it still retains superior resistance compared to other alloys. Meanwhile, the 20Ni80Cr sample exhibits a wear loss of 44 mg at 20 h, which is only slightly lower than its 46 mg wear loss in the non-cavitation condition, indicating a marginal protective effect of cavitation inducers.

The presence of cavitation inducers seems to reduce the wear rate of some materials (such as AR and 20Ni80Cr), while having minimal effect on others (such as 40Ni60Cr and 50Ni50Cr). The 50Ni50Cr alloy continues to show the highest wear resistance, reinforcing its suitability for applications requiring strong durability. The data suggests that cavitation may influence wear mechanisms differently for each material, possibly altering erosion patterns. However, the general trend remains that a balanced Ni-Cr composition, as seen in 50Ni50Cr, provides the best resistance to wear, even under cavitation conditions.

The graph in Figure 7 represents the wear loss (mg) of different materials over time in the presence of cavitation inducers, showing a gradual increase in wear for all samples. AR (As Received) still exhibits the highest wear loss, indicating poor wear resistance under cavitation conditions. 50Ni50Cr continues to show the lowest wear loss, proving its superior durability even with cavitation

10.3389/fmats.2025.1671031

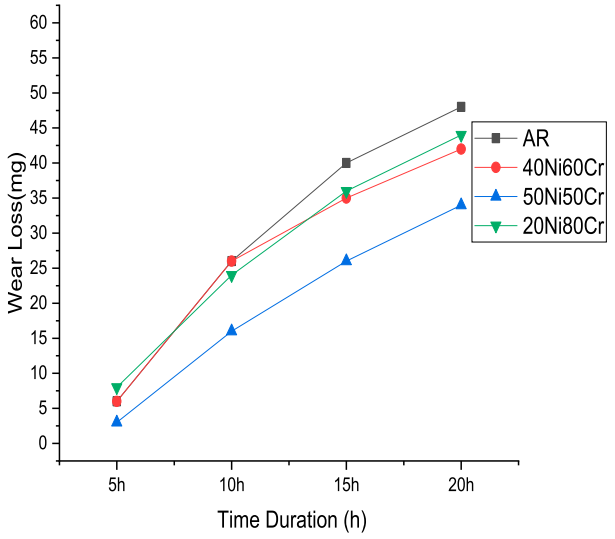

FIGURE 7
Variation of wear loss with cavitation inducers.

TABLE 3 Percentage change in wear loss between with and without cavitation inducers.

Sample	5 h (%)	10 h (%)	15 h (%)	20 h (%)
AR	+20.00	−25.71	−13.04	−14.29
40Ni60Cr	+500.00	+44.44	0.00	−2.33
50Ni50Cr	+50.00	+6.67	+4.00	+17.24
20Ni80Cr	+33.33	−20.00	−5.26	−4.35

inducers. 40Ni60Cr and 20Ni80Cr display similar wear trends, but 20Ni80Cr experiences slightly more wear over time. Overall, cavitation inducers do not drastically alter the ranking of material performance, with 50Ni50Cr remaining the most wear resistant.

5.2 Comparison of wear loss data with and without cavitation inducers

The comparison of wear loss data with and without cavitation inducers reveals key differences in material performance under different conditions. Generally, all materials exhibit increasing wear over time, but the rate and extent of wear vary significantly depending on their composition. The presence of cavitation inducers appears to reduce wear in some materials, such as the as-received (AR) sample and 20Ni80Cr, while having minimal impact on others, like 40Ni60Cr and 50Ni50Cr. This suggests that cavitation may alter erosion patterns in certain materials, possibly influencing how surface degradation occurs.

The AR sample, which initially shows the highest wear loss, exhibits a notable reduction when cavitation inducers are present, with wear at 20 h decreasing from 56 mg to 48 mg. This indicates that cavitation may mitigate some of the wear mechanisms affecting this material. Similarly, the 20Ni80Cr sample experiences a slight improvement, with a decrease in wear loss decreasing from 46 mg to 44 mg at 20 h, though it still shows significant material degradation. In contrast, the 40Ni60Cr sample shows nearly identical wear performance in both conditions, with 43 mg wear loss without cavitation and 42 mg with cavitation, indicating that cavitation does not significantly alter its wear resistance.

The 50Ni50Cr alloy consistently demonstrates the best wear resistance, making it the most durable material tested. Without cavitation, it has the lowest wear loss at 29 mg at 20 h, and although cavitation slightly increases its wear to 34 mg, it still outperforms all other materials. This suggests that while cavitation has a small effect on its durability, the balanced Ni-Cr composition provides excellent resistance to wear, regardless of external conditions. Nickel contributes to toughness and ductility, while chromium enhances hardness and passivation. At an equal ratio (50Ni50Cr), the alloy benefits from a synergistic effect chromium provides surface stability against erosive attack, while nickel improves crack blunting and plastic accommodation during impact. Thermodynamically, this balance reduces localized stress concentration and stabilizes the austenitic structure, thereby lowering the net wear rate compared to Ni-rich or Cr-rich counterparts.

The presence of cavitation inducers does not always accelerate wear in some cases, it reduces material degradation, particularly in the AR and 20Ni80Cr samples. However, the 50Ni50Cr alloy remains the superior choice for wear resistance in both conditions, reinforcing its suitability for applications where durability is essential. These findings highlight the importance of material selection in wear-intensive environments, where cavitation effects should be carefully considered based on material composition.

5.3 Percentage change in wear loss

The percentage-change analysis of wear loss with cavitation inducers reveals varying behaviors across different materials, as shown in Table 3. At the 5-h mark, both AR and 20Ni80Cr show moderate increases in wear (20% and 33.33%, respectively), while 40Ni60Cr exhibits a significant 500% jump, suggesting early-stage susceptibility to cavitation for these alloys. However, from 10 h onward, AR and 20Ni80Cr both display negative percentage changes (e.g., −25.71% and −20% at 10 h), indicating reduced wear compared to tests without cavitation inducers over longer durations. In contrast, 50Ni50Cr consistently shows positive percentage changes (reaching +17.24% at 20 h), implying that cavitation slightly accelerates wear for this otherwise highly wear-resistant alloy. Meanwhile, 40Ni60Cr's wear stabilizes after the initial spike, transitioning from +44.44% at 10 h to −2.33% at 20 h, indicating that cavitation has a diminishing impact over time. Overall, these findings suggest that cavitation can either exacerbate or mitigate wear depending on both the specific alloy composition and the duration of exposure, with 50Ni50Cr remaining the most wear-resistant despite a mild increase under cavitation conditions.

5.4 SEM analysis of worn-out surface

This Scanning Electron Micrograph (SEM) Figure 8 highlights the highly roughened eroded surface with pronounced irregular

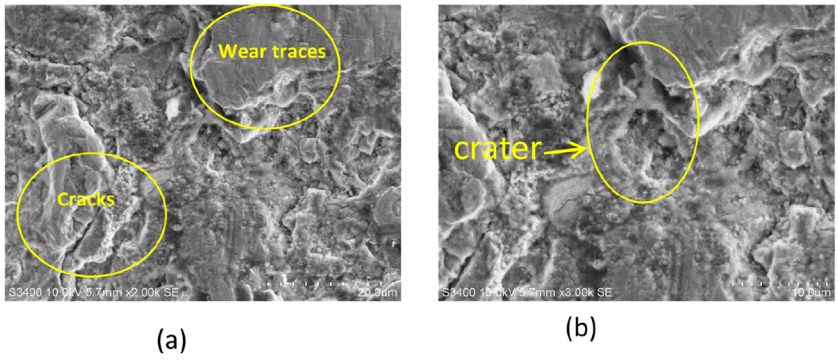

FIGURE 8
SEM Image with cavitation inducers of 50Ni50Cr specimen. **(a)** 20 μm. **(b)** 10 μm.

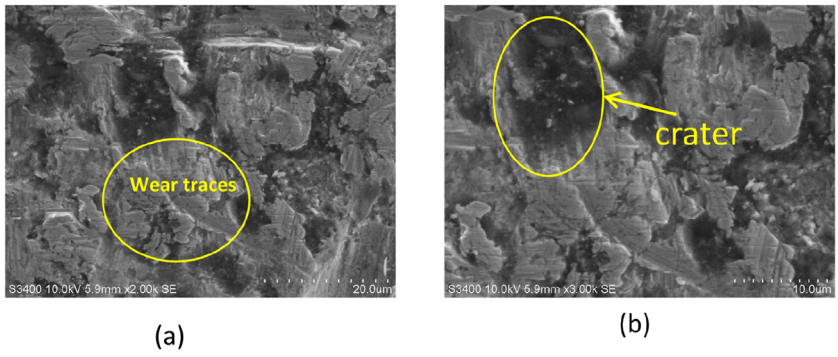

FIGURE 9
SEM Image without cavitation inducers of 50Ni50Cr specimen. **(a)** 20 μm. **(b)** 10 μm.

features on the order of micrometers (the scale bar indicates 10 μm) of 50Ni50Cr specimen with cavitation inducers. The texture appears composed of overlapping plastically deformed regions, indicating that the surface has undergone substantial erosive wear. In some areas, slight cracking can be observed, potentially indicative of localized stress concentrations. The overall morphology features jagged contours and uneven topography, which is a characteristic of severe surface damage that may arise from processes such as cavitation erosion and abrasive wear. Such microstructural details are often used to infer the dominant wear mechanisms that guide the improvements in surface treatment processes.

The SEM image shown in Figure 9 shows the rough and irregular surface with fragmented and layered features, severe mechanical wear, or erosion conditions of the specimen 50Ni50Cr without cavitation inducers (the scale bar indicates 10 μm). The bright and dark contrast areas suggest variations in local topography with protrusions and depressions in the specimen. Some regions display lamellar-like flakes or platelets, which indicates that portions of the surface may have fractured under stress. In addition, the presence of microscopic voids could highlight the local crack initiation due to cavitation effects. The morphology reflects a highly damaged surface consistent with a high rate of erosive forces acting over the period.

Comparing SEM images, exhibit severely worn-out surfaces and highly irregular surfaces, indicating extensive erosive damage. In Figure 8, the surface appears to have a more granular texture with overlapping plastically deformed regions and occasional fissures. On the other side, the second (Figure 9) shows more pronounced lamellar or flake-like structures, suggesting that material may have peeled away in layers under stress. While both reveal jagged contours and evidence of surface degradation while the first image displays slightly larger, more distinct fragments, implying a potentially more advanced stage of wear. Despite these minor distinctions, both Figures confirm significant damage likely resulting from similar wear mechanisms such as cavitation erosion and abrasive impact.

In comparison, all the specimens exhibited the same type of wear mechanisms, and their worn surfaces appeared almost identical, making it difficult to highlight clear morphological differences. However, the 50Ni–50Cr specimen demonstrated a noticeably lower erosion rate compared to the other specimens, indicating better wear resistance despite the similar surface features.

6 Conclusion

The overall analysis reveals that the influence of cavitation inducers on wear loss is multifaceted and highly dependent on both the alloy composition and the exposure duration. Initially, the presence of cavitation inducers appears to induce a notable spike

in wear for some materials; for instance, 40Ni60Cr experiences a dramatic increase in wear loss at the 5-h mark, indicating a heightened early susceptibility to cavitation effects. Conversely, materials like AR and 20Ni80Cr also show an initial increase, but this is followed by a reduction in wear loss over longer periods, suggesting that these materials may develop some form of protective mechanism or stabilization over time under cavitation conditions.

In contrast, the 50Ni50Cr alloy consistently exhibits the lowest wear loss, even though it experiences a slight increase when cavitation inducers are present. This performance underscores the inherent durability of 50Ni50Cr and suggests that its balanced nickel-chromium composition is effective in resisting the detrimental effects of cavitation, making it a promising candidate for applications in wear-intensive environments. Overall, the data implies that while cavitation can either exacerbate or mitigate wear depending on the material and the time frame, 50Ni50Cr remains the most reliable in terms of long-term wear resistance. This nuanced behavior highlights the need for a tailored approach in material selection, especially in scenarios where both short-term and long-term durability under cavitation conditions are critical considerations.

Data availability statement

The original contributions presented in the study are included in the article/supplementary material, further inquiries can be directed to the corresponding author.

Author contributions

PM: Formal Analysis, Validation, Writing – original draft. AH: Data curation, Methodology, Supervision, Writing – review and editing. VK: Conceptualization, Project administration, Supervision, Visualization, Writing – original draft. MA: Formal Analysis, Funding acquisition, Resources, Validation, Writing – review and editing. UD: Conceptualization, Investigation, Supervision, Visualization, Writing – review and editing.

Funding

The author(s) declare that no financial support was received for the research and/or publication of this article.

Conflict of interest

The authors declare that the research was conducted in the absence of any commercial or financial relationships that could be construed as a potential conflict of interest.

Generative AI statement

The author(s) declare that no Generative AI was used in the creation of this manuscript.

Any alternative text (alt text) provided alongside figures in this article has been generated by Frontiers with the support of artificial intelligence and reasonable efforts have been made to ensure accuracy, including review by the authors wherever possible. If you identify any issues, please contact us.

Publisher's note

References

Akisin, C. J., Venturi, F., and Bai, M (2021). Microstructure, mechanical and wear resistance properties of low-pressure cold-sprayed Al-7 Mg/Al_2O_3 and Al-10 Mg/Al_2O_3 composite coatings. *Emergent Mater* 4, 1569–1581. doi:10.1007/s42247-021-00293-4

Algoburi, A., Ahmed, R., and Kumar, V. (2024). Cavitation erosion in HVOF thermally sprayed WC-NiCrBSi coatings. *Therm. Spray. Conf. Proc. Milan. Italy* 84864, 248–255. doi:10.31399/asm.cp.itsc2024p0248

Amarendra, H. J., Prathap, M. S., Karthik, S., Darshan, B. M., Devaraj, Girish, P. C., et al. (2017). Combined slurry and cavitation erosion resistance of HVOF thermal spray coated stainless steel. *Mater. Today Proc.* 4 (2), 465–470. doi:10.1016/j.matpr.2017.01.046

Finnie, I. (1960). Erosion of surfaces by solid particles. *Wear* 3 (2), 87–103. doi:10.1016/0043-1648(60)90055-7

Grewal, H. S., Arora, H. S., Agrawal, A., Singh, H., and Mukherjee, S. (2013a). Slurry erosion of thermal spray coatings: effect of sand concentration. *Procedia Eng.* 68, 484–490. doi:10.1016/j.proeng.2013.12.210

Grewal, H. S., Agrawal, A., and Singh, H. (2013b). Design and development of high-velocity slurry erosion test rig using CFD. *J. Mater. Eng. Perform.* 22, 152–161. doi:10.1007/s11665-012-0219-y

Hong, S., Wu, Y., Zhang, J., Zheng, Y., Qin, Y., Gao, W., et al. (2015). Cavitation erosion behavior and mechanism of HVOF sprayed WC-10Co-4Cr coating in 3.5 wt% NaCl solution. *Trans. Indian Inst. Metals* 68, 151–159. doi:10.1007/s12666-014-0440-5

Krastev, D. (2012). Improvement of corrosion resistance of steels by surface modification. *Corros. Resist. Shih*. doi:10.5772/33144

Kumar, K., Kumar, S., Singh, G., Singh, J. P., and Singh, J. (2017). Erosion wear investigation of HVOF sprayed WC-10Co4Cr coating on slurry pipeline materials. *Coatings* 7 (4), 54. doi:10.3390/coatings7040054

Kumar, R., Kumar, S., and Mudgal, D. (2022). Silt erosion performance of high velocity oxy fuel-(HVOF) sprayed Al2O3–Cr2O3 composite coatings on turbine steel. *Industrial Lubr. Tribol.* 74 (5), 572–579. doi:10.1108/ilt-08-2021-0346

Lekka, M., Kouloumbi, N., Gajo, M., and Bonora, P. L. (2005). Corrosion and wear resistant electrodeposited composite coatings. *Electrochimica Acta* 50 (23), 4551–4556. doi:10.1016/j.electacta.2004.11.067

Li, Y., Burstein, G. T., and Hutchings, I. M. (1995). The influence of corrosion on the erosion of aluminium by aqueous silica slurries. *Wear* 186-187 (2), 515–522. doi:10.1016/0043-1648(95)07181-4

Lin, J., Hong, S., Zheng, Y., Sun, W., Zhang, Z., Kang, M., et al. (2022). Cavitation–silt erosion behavior and failure mechanism of an HVOF-sprayed WC-Cr_3C_2-Ni coating for offshore hydraulic machinery. *J. Mar. Sci. Eng.* 10 (10), 1341. doi:10.3390/jmse10101341

Maurer, C., and Schulz, U. (2014). Solid particle erosion of thick PVD coatings on CFRP. *Wear* 317 (1-2), 246–253. doi:10.1016/j.wear.2014.05.016

Milanti, A., Koivuluoto, H., Vuoristo, P., Bolelli, G., Bozza, F., and Lusvarghi, L. (2014). Microstructural characteristics and tribological behavior of HVOF-sprayed novel Fe-based alloy coatings. *Coatings* 4 (1), 98–120. doi:10.3390/coatings4010098

Ramanath, M. N., Chikmath, L., and Murthy, H. (2024). Effect of cold-working on corrosion induced damage in lug joints. *Def. Technol.* 36, 175–182. doi:10.1016/j.dt.2023.10.008

Ramesh, C. S., Keshavamurthy, R., Channabasappa, B. H., and Pramod, S. (2010). Friction and wear behavior of Ni–P coated Si3N4 reinforced Al6061 composites. *Tribol. Int.* 43 (3), 623–634. doi:10.1016/j.triboint.2009.09.011

Ramesh, C. S., Devaraj, D. S., Keshavamurthy, R., and Sridhar, B. R. (2011). Slurry erosive wear behaviour of thermally sprayed Inconel-718 coatings by APS process. *Wear* 271 (9-10), 1365–1371. doi:10.1016/j.wear.2011.01.057

Santa, J. F., Espitia, L. A., Blanco, J. A., Romo, S. A., and Toro, A. (2009). Slurry and cavitation erosion resistance of thermal spray coatings. *Wear* 267 (1-4), 160–167. doi:10.1016/j.wear.2009.01.018

Santacruz, G., ShigueakiTakimi, A., Vannucchi de Camargo, F., Pérez Bergmann, C., and Fragassa, C. (2019). Comparative study of jet slurry erosion of martensitic stainless steel with tungsten carbide HVOF coating. *Metals* 9 (5), 600. doi:10.3390/met9050600

Sapate, S. G., Tangselwar, N., Paul, S. N., Rathod, R. C., Mehar, S., Gowtam, D. S., et al. (2021). Effect of coating thickness on the slurry erosion resistance of HVOF-sprayed WC-10Co-4Cr coatings. *J. Therm. spray Technol.* 30, 1365–1379. doi:10.1007/s11666-021-01190-2

Seitov, B., Kurbanbekov, S., Baltabayeva, D., Kakimzhanov, D., Katpayeva, K., Temirbekov, A., et al. (2025). Review of physical and mechanical properties, morphology, and phase structure in Cr3C2-NiCr composite coatings sprayed by HVOF method. *Coatings* 15 (4), 479. doi:10.3390/coatings15040479

Senapati, P., Sutar, H., Murmu, R., and Gupta, S. (2022). "Slurry erosion behaviour of HVOF-sprayed NiAl composite coating," in *In recent advances in mechanical engineering: select Proceedings of ICRAMERD 2021*, 623–629.

Shunin, Y. N., and Kiv, A. E. (2012). "Nanodevices and nanomaterials for ecological security. The Nato science for peace and security," in *Series B: physics and biophysics*.

Singh, R., Kumar, M., Kumar, D., and Mishra, S. K. (2012). Erosion and corrosion behavior of laser cladded stainless steels with tungsten carbide. *J. Mater. Eng. Perform.* 21, 2274–2282. doi:10.1007/s11665-012-0170-y

Suresh Babu, P., Bikramjit, B., and Sundararajan, G. (2011). The influence of erodent hardness on the erosion behavior of detonation-sprayed WC-12Co coatings. *Wear* 270 (11), 903–913. doi:10.1016/j.wear.2011.02.019

Taşan, Y. C., de Rooij, M. B., and Schipper, D. J. (2005). Measurement of wear on asperity level using image-processing techniques. *Wear* 258 (1-4), 83–91. doi:10.1016/j.wear.2004.05.018

Thakur, L., and Arora, N. (2013). A comparative study on slurry and dry erosion behaviour of HVOF sprayed WC–CoCr coatings. *Wear* 303 (1-2), 405–411. doi:10.1016/j.wear.2013.03.028

Tian, Y., Yang, R., Gu, Z., Zhao, H., Wu, X., Dehaghani, S. T., et al. (2022). Ultrahigh cavitation erosion resistant metal-matrix composites with biomimetic hierarchical structure. *Compos. Part B Eng.* 234, 109730. doi:10.1016/j.compositesb.2022.109730

Vignesh, S., Balasubramanian, V., Sridhar, K., and Thirumalaikumarasamy, D. (2019). Slurry erosion behavior of HVOF-sprayed amorphous coating on stainless steel. *Metallogr. Microstruct. Analysis* 8, 462–471. doi:10.1007/s13632-019-00552-1

Wang, X., Fang, M., Zhang, L. C., Ding, H., Liu, Y. G., Huang, Z., et al. (2013). Solid particle erosion of alumina ceramics at elevated temperature. *Mater. Chem. Phys.* 139 (2-3), 765–769. doi:10.1016/j.matchemphys.2013.02.029

Xu, X., Mi, G., Chen, L., Xiong, L., Jiang, P., Shao, X., et al. (2017). Research on microstructures and properties of Inconel 625 coatings obtained by laser cladding with wire. *J. alloys Compd.* 715, 362–373. doi:10.1016/j.jallcom.2017.04.252

Yang, X., Zhang, J., and Li, G. (2018). Cavitation erosion behaviour and mechanism of HVOF-sprayed NiCrBSi–(Cr3C2–NiCr) composite coatings. *Surf. Eng.* 34 (3), 211–219. doi:10.1080/02670844.2016.1258770

Yi, J., Miao, Q., Liang, W., Liu, Y., Qi, Y., Ding, Z., et al. (2022). A functionally graded coating from ZrN to Ti: experimental characterization, erosion behavior and design concept. *Surf. coatings Technol.* 432, 128093. doi:10.1016/j.surfcoat.2022.128093

Zafar, S., and Sharma, A. K. (2014). Development and characterisations of WC–12Co microwave clad. *Mater. Charact.* 96, 241–248. doi:10.1016/j.matchar.2014.08.015

Zhao, Y., Yu, T., Chen, L., Chen, Y., Guan, C., and Sun, J. (2020). Microstructure and wear resistance behavior of Ti–C–B4C-reinforced composite coating. *Ceram. Int.* 46 (16), 25136–25148. doi:10.1016/j.ceramint.2020.06.300